

FIG. 1. TEOS signal of a superlattice with 36 meV miniband width at a reverse bias voltage of -2.9 V. The excitation density is 2×10^9 cm^{-2} .

spectral width of 40 meV at a repetition rate of 82 MHz. TEOS is a conventional pump-probe technique in transmission geometry, where a circularly polarized probe pulse is analyzed polarization-sensitively as a function of the time delay with respect to a stronger, linearly polarized pump pulse. The detected transmission changes are in first order proportional to changes in the polarization P_z directed parallel to the growth direction of the superlattice.¹¹ Bloch oscillations appear in the signal due to the macroscopic dipole associated with the coherent center-of-mass motion of electrons relative to localized holes.¹¹ Additionally, changes in P_z can be observed which originate from an incoherent current through the SL thus screening the applied electric field.

The SL consists of 35 periods of 67 Å wide GaAs wells and 17 Å wide $\text{Al}_{0.3}\text{Ga}_{0.7}\text{As}$ barriers. The SL is placed between intrinsic $\text{Al}_{0.3}\text{Ga}_{0.7}\text{As}$ buffers. This structure of a total intrinsic region of 1 μm is grown on an n -type doped substrate. An external bias can be applied via an Ohmic contact on the substrate and a semitransparent Cr/Au Schottky contact on top of the sample. For transmission measurements, the substrate has been partially removed by wet etching. For the lowest electronic miniband, a width of 36 meV is calculated using the Kronig-Penney model. The small width of the heavy-hole (hh) miniband of 2.5 meV leads to a strong localization of the wave functions even at small electric fields. The WS ladder in the SL has been measured in photocurrent spectroscopy at 10 K. At 300 K, the WS ladder is not resolved due to broadening of the excitonic transitions. The laser wavelength is centered at 845 nm between the hh to 0 and the hh to -1 WS transition at higher fields applied. At lower fields, where the splitting of WS states is well below the spectral width of the laser pulse, a whole set of WS transitions is excited.

Figure 1 shows a typical TEOS signal for a reverse bias voltage of -2.9 V at an excitation density of 2×10^9 carriers per cm^2 at room temperature. The signal consists of a step-like contribution at zero time delay followed by a strong oscillating modulation due to the excitation of BO's. The rise of the TEOS signal additionally monitors incoherent electric field changes in the SL due to carrier transport through the structure. This current is a direct measure of Bloch electrons which have undergone a scattering process. The simultaneously recorded FWM signal (not shown) only exhibits an autocorrelation peak at zero time delay indicating that the

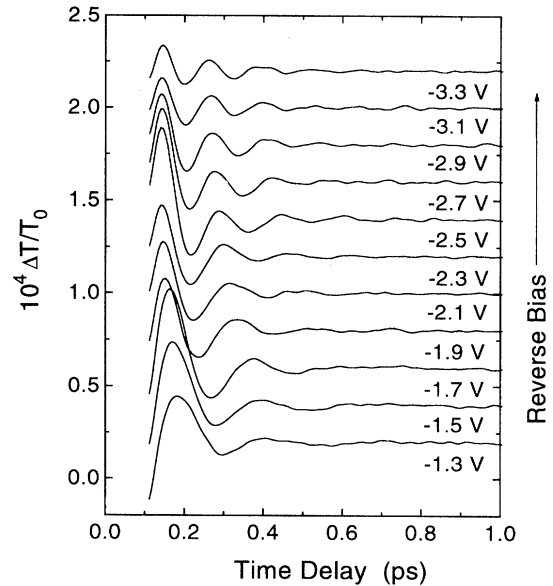


FIG. 2. Extracted oscillatory contributions from TEOS data at different reverse bias voltages applied.

dephasing of the nonlinear interband polarization is by far too fast for allowing the observation of BO's. The field changes observed within the dephasing time of the BO's will influence both their frequency and their dephasing. The field screening will introduce a redshift of the BO frequency with time due to a reduction of the WS splitting. More important, the field changes within the SL will not be homogeneous due to an inhomogeneous excitation density associated with the absorption profile of the laser pulse and due to different mobilities of electron and holes. Such strongly inhomogeneous field distributions have been observed after pulsed excitation of a biased GaAs film.²⁵ In the SL, these inhomogeneous fields result in a superposition of BO's with different frequencies leading to an increase in "dephasing" time.

In Fig. 2 the BO induced signals numerically extracted from TEOS data are shown for several reverse bias voltages applied to the sample. The increase of frequency with increasing voltage is clearly visible. The dephasing time as determined by numerical fits to the data is approximately constant over the whole voltage range ($\tau=130$ fs). The fits are based on a monoexponential decaying sine. For some bias values the decay of the amplitude is clearly not monoexponential. This observation is attributed to the inhomogeneity of the electric fields. In Fig. 3, the Fourier transforms of some time-domain data are shown. The width of the Fourier spectra does not change significantly over the frequency range depicted. The asymmetric shape of the spectra indicate a nonexponential dephasing. We estimate the accuracy in the determination of the peak position of the BO's to be approximately 0.5 THz.

Figure 4 shows the frequencies as obtained by the Fourier transform of TEOS data versus the reverse bias applied. The range of tunability covers approximately 4 THz. The dependence of the frequency on the voltage is linear as expected for electronic BO's. The lowest frequency of 4.5 THz corresponds to an energy of 18.5 meV, which is well below the

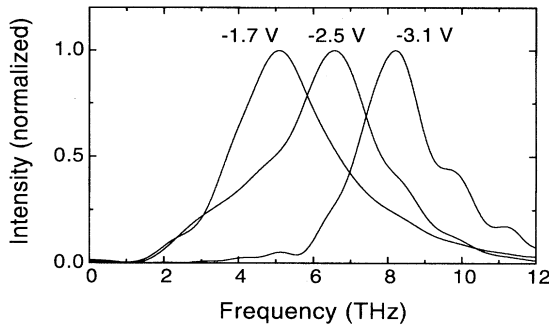


FIG. 3. Fourier transform of the time-domain data at -1.7 V, -2.5 V, and -3.1 V reverse bias.

thermal energy of $kT=25$ meV. This lower limit is not only determined by the dephasing time, but also strongly dependent on the spectral width of the laser pulse (40 meV). At a WS splitting below 20 meV the laser excites several WS transitions with positive and negative index according to their absorption strength. The superposition of the, e.g., $+1$ and -1 WS transition leads to a breathing motion of the wave packet,³¹ which is not associated with a net intraband polarization and does therefore not appear in the TEOS signal. The upper frequency observed of 8 THz corresponds to the frequency of the TO phonon of GaAs. A linear fit to the frequencies gives a slope of (2.1 ± 0.3) THz/V. The theoretical slope expected for the sample parameters is $ed/hl_{\text{intr}}=2.29$ THz/V, where l_{intr} is the length of the total intrinsic region of the SL structure. So the difference in the slopes is within the experimental error. For excitonic quantum beats as observable in FWM experiments at low temperatures, a smaller slope is expected due to the field dependence of the excitonic binding energies.²⁰ This effect is based on the increasing exciton binding energy of the hh to 0 WS transition due to increasing localization of the electronic wave function at higher field and a decrease of the binding energy of the “indirect” hh to -1 WS transition, thus the excitonic BO frequency should be about 1 THz below eFd/h when the electric field is equal to the miniband width divided by ed . Therefore the agreement between the theoretical and the experimental frequency/field relation shows that the os-

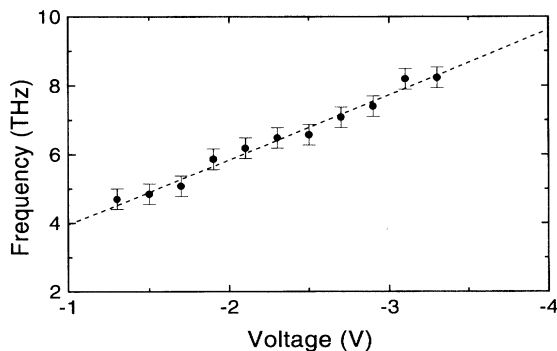


FIG. 4. Frequency of Bloch oscillations versus voltage applied to the superlattice. The straight line is a linear fit to the data with a slope of 2.1 ± 0.3 THz/V.

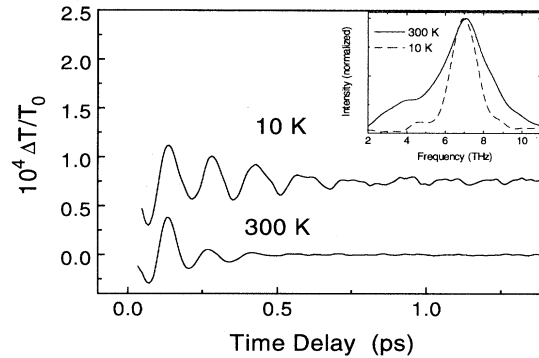


FIG. 5. Comparison of Bloch oscillations at 10 K (upper curve) and 300 K (lower curve) at the same excitation density. The inset shows the Fourier transforms.

cillations are due to electrons in continuum states. A deviation from the semiclassical frequency/field relation for BO's is expected when the BO's are in resonance with the LO phonon.²⁶ Up to now, coherent oscillations observed in GaAs in this frequency range originate from coherent lattice vibrations.²⁷

In Fig. 5 we compare the BO induced TEOS signal at room temperature with BO's recorded at a lattice temperature of 10 K in the same sample. For the low temperature experiment, the sample is placed in a cryostat and the laser wavelength is adjusted to the shift of the band edge to 800 nm. The excitation densities are approximately the same for both experiments as indicated by the same amplitude of the BO's at time-delay zero. The two curves are chosen at bias voltages, where the frequency in both experiments matches. The reverse bias has to be adjusted to higher values at low temperatures, since the frequency/voltage relation deviates from the theoretical expected value due to cw accumulation of carriers at the $\text{Al}_{0.3}\text{Ga}_{0.7}\text{As}$ cladding barriers of the SL at the high laser repetition rate. At room temperature, this effect is not observed since thermionic emission of carriers over the cladding barriers suppresses the accumulation effect. The dephasing time of the BO's at 10 K is 370 fs. Hence, the dephasing time at 300 K is decreased by a factor of 3, as it is also clearly observed in the different widths of the Fourier spectra. We like to note that in a SL with a narrower miniband width of 18 meV we have observed a dephasing time of 2.8 ps at 10 K and excitation with a laser pulse of smaller bandwidth (22 meV).¹¹ We attribute the longer dephasing time (i) to the more homogeneous excitation conditions obtained with the narrower laser spectrum and (ii) to a better sample quality.²⁸

Several theoretical and experimental works considered the dephasing of BO's.^{11,19,29-31} von Plessen *et al.* pointed out that BO's should not be observable in SL's with miniband widths exceeding the energy of an optical phonon.³⁰ However, our results demonstrate the observation of BO's in a wide miniband SL even with frequencies up to the TO phonon. The decrease of the dephasing time by a factor of 3 when increasing the lattice temperature from 10 K to room temperature is surprisingly small. In FWM experiments, the excitonic dephasing time has been determined to increase by more than a factor of 10 from 10 K to 300 K due to the

increase of scattering with thermally occupied acoustic and optical phonons.²¹ This confirms the assumption of an exceptionally slow dephasing of continuum states.²⁰ The difference in the dephasing time of the electronic and the excitonic wave packets at a given temperature can be principally explained by the different interactions responsible for dephasing of the intraband and interband polarization, respectively. The excitonic interband coherence is destroyed by interactions in both valence and conduction bands, while the intraband polarization is only influenced by scattering processes in one band. However, the temperature dependence of the dephasing time observed in TEOS is still surprisingly weak, when we assume the same temperature dependence for phonon scattering rates of excitons as for electrons. One further dephasing mechanism increasing with temperature is the effect of transient inhomogeneous fields. Due to a reduced scattering of Bloch wave packets at low temperatures, the internal field remains more homogeneous due to a reduced incoherent current. Clearly, the observed temperature dependence of the intraband dephasing time requires further investigation. One possibility to resolve this discrepancy is that the macroscopic phase of the 'electronic wave packets oscillating perpendicular to the layers of the SL is partially maintained under certain scattering processes involving a momentum exchange perpendicular to the layers.

In conclusion, we reported on the observation of coherently excited Bloch oscillations in a GaAs/Al_{0.3}Ga_{0.7}As superlattice at room temperature. The dephasing time of the Bloch oscillations performed by electrons in continuum states exceeds 100 fs at 300 K, which is only a factor of 3 faster than at 10 K in the same sample under the same excitation conditions. The frequency of the oscillations can be tuned in the range of 4.5 THz to 8 THz. These observations open the way for a future application of Bloch oscillations. The observation of THz emission by Bloch oscillations at 300 K should be possible, if the detection bandwidth of the antennas exceeds 4 THz.

We are indebted to P. Leisching for valuable discussions. We thank H. J. Bakker and R. Schwedler for carefully reading the manuscript, and G.C. Cho for assistance with the laser system. F. Brüggemann is acknowledged for performing cw-photocurrent characterization. This work was supported by the Volkswagen Stiftung.

- ¹ *Coherent Optical Interactions in Semiconductors*, Vol. 330 of *NATO Advanced Study Institute, Series B: Physics*, edited by R. T. Philips (Plenum Press, New York, 1994), and contributions therein.
- ² L. Leo, T. C. Damen, J. Shah, E. O. Göbel, and K. Köhler, *Appl. Phys. Lett.* **57**, 19 (1990).
- ³ P. C. M. Planken, M. C. Nuss, I. Brenner, K. W. Goosen, M. S. C. Luo, S. L. Chuang, and L. Pfeifer, *Phys. Rev. Lett.* **69**, 3800 (1992).
- ⁴ K. Leo, T. C. Damen, J. Schah, and K. Köhler, *Phys. Rev. B* **42**, 11 359 (1990).
- ⁵ K. Leo, J. Shah, E. O. Göbel, T. C. Damen, S. Schmitt-Rink, W. Schäfer, and K. Köhler, *Phys. Rev. Lett.* **66**, 201 (1991).
- ⁶ H. G. Roskos, M. C. Nuss, J. Shah, K. Leo, D. A. B. Miller, A. M. Fox, S. Schmitt-Rink, and K. Köhler, *Phys. Rev. Lett.* **68**, 2216 (1992).
- ⁷ D. J. Lovering, R. T. Philips, G. J. Denton, and G. W. Smith, *Phys. Rev. Lett.* **68**, 1880 (1992).
- ⁸ J. Feldmann, K. Leo, J. Shah, D. A. B. Miller, J. E. Cunningham, S. Schmitt-Rink, T. Meier, G. von Plessen, A. Schulze, and P. Thomas, *Phys. Rev. B* **46**, 7252 (1992).
- ⁹ K. Leo, P. Haring Bolivar, F. Brüggemann, R. Schwedler, and K. Köhler, *Solid State Commun.* **84**, 943 (1992).
- ¹⁰ C. Waschke, H. G. Roskos, R. Schwedler, K. Leo, H. Kurz, and K. Köhler, *Phys. Rev. Lett.* **70**, 3319 (1993).
- ¹¹ T. Dekorsy, P. Leisching, K. Köhler, and H. Kurz, *Phys. Rev. B* **50**, 8106 (1994).
- ¹² J. Kuhl, E. J. Mayer, G. Smith, R. Eccleston, D. Bennhardt, P. Thomas, K. Bott, and O. Heller, in *Coherent Optical Interactions in Semiconductors* (Ref. 1).
- ¹³ E. E. Mendez, F. Agulló-Rueda, and J. M. Hong, *Phys. Rev. Lett.* **60**, 2426 (1988).
- ¹⁴ P. Voisin, J. Bleuse, C. Bouche, S. Gaillard, C. Alibert, and A. Regreny, *Phys. Rev. Lett.* **61**, 1639 (1988).
- ¹⁵ F. Bloch, *Z. Phys.* **52**, 555 (1928).
- ¹⁶ C. Zener, *Proc. R. Soc. London Ser. A* **145**, 523 (1934).
- ¹⁷ L. Esaki and R. Tsu, *IBM J. Res. Dev.* **61**, 61 (1970).
- ¹⁸ G. Bastard and R. Ferreira, in *Spectroscopy of Semiconductor Microstructures, NATO Advanced Study Institute, Series B: Physics*, edited by G. Fasol and A. Fasolino (Plenum, New York, 1989), p. 333.
- ¹⁹ P. Leisching, P. Haring Bolivar, W. Beck, Y. Dhaibi, K. Leo, K. Köhler, and H. Kurz, *Phys. Rev. B* **50**, 14 389 (1994).
- ²⁰ P. Leisching, T. Dekorsy, H. J. Bakker, H. Kurz, and K. Köhler, *Phys. Rev. B* (to be published).
- ²¹ D.-S. Kim, J. Shah, J. E. Cunningham, T. C. Damen, W. Schäfer, M. Hartmann, and S. Schmitt-Rink, *Phys. Rev. Lett.* **68**, 1006 (1992).
- ²² K. Fujiwara, *Jpn. J. Appl. Phys.* **28**, L1718 (1989).
- ²³ E. E. Mendez, F. Agulló-Rueda, and J. M. Hong, *Appl. Phys. Lett.* **56**, 2545 (1990).
- ²⁴ K. Kawashima, K. Fujiwara, T. Yamamoto, M. Sigeta, and K. Kobayashi, *Jpn. J. Appl. Phys.* **30**, L793 (1991).
- ²⁵ H. Heesel, S. Hunsche, H. Mikkelsen, T. Dekorsy, K. Leo, and H. Kurz, *Phys. Rev. B* **47**, 16 000 (1993).
- ²⁶ T. Dekorsy, H. Kurz, and K. Köhler (unpublished).
- ²⁷ G. C. Cho, W. Kütt, and H. Kurz, *Phys. Rev. Lett.* **65**, 764 (1990); T. Dekorsy, T. Pfeifer, W. Kütt, and H. Kurz, *Europhys. Lett.* **23**, 223 (1993).
- ²⁸ The zero-field luminescence linewidths of both samples at 10 K are 0.8 meV (18 meV sample, homogeneously broadened) and 1.5 meV (36 meV sample, inhomogeneously broadened).
- ²⁹ A. M. Bouchard and M. Luban, *Phys. Rev. B* **47**, 6815 (1993).
- ³⁰ G. von Plessen, T. Meier, J. Feldmann, E. O. Göbel, P. Thomas, K. W. Goosen, J. M. Kuo, and R. F. Kopf, *Phys. Rev. B* **49**, 14 058 (1994).
- ³¹ M. Dignam, J. E. Sipe, and J. Shah, *Phys. Rev. B* **49**, 10 502 (1994).